CHAPTER 4

Study of acute homeostatic responses to a carcinogen in rat colonic epithelium

4.1. Time course study

4.1.1. Aims

The purpose of this study was to observe the acute homeostatic responses that take place in the colon in response to an insult of an alkylating carcinogen over time. With this information, it is hoped that the relationship between the formation of DNA damage and the initiation of removal mechanisms can be better understood. Furthermore, this study also provided the opportunity to demonstrate the effectiveness of the newly established O^6medG immunohistochemical assay.

The specific aims of this particular study include;

1. To measure the pattern of O^6medG formation in colonic epithelial cells of rats following an insult of the alkylating carcinogen over a set time course of 48h.

2. To also measure the rates of apoptosis and cell proliferation in colonic epithelial cells over the time course of 48h.

3. To compare these responses and establish a pattern of acute colonic DNA damage and removal in the rat-AOM model.

4.1.2. Experimental rationale

It has been shown previously that that the acute apoptotic response in rat colonic epithelium peaks at approximately 6-8h post AOM administration. This has been supported by our own experiments and also by other external publications. Internal experiments have failed to observe a later 'second wave' of apoptosis, an observation that has been reported by Merritt *et al*. [172] in rat small intestine

when using radiation as a source of DNA damage. This second wave was observed approximately 48h following irradiation treatment. Similarly, *in vitro* experiments have also identified a later onset of apoptosis 72h after exposure to an alkylating agent [97].

Popular theory suggests that the onset of this delayed apoptosis is indirectly related to the formation of O^6medG adducts. It is proposed that the initiation of apoptosis via O^6medG adducts requires two rounds of DNA replication and the formation of double strand breaks to occur. In short, the DNA mispairs created by O^6medG lesions after one round of DNA synthesis are subjected to defective MMR [95]. This in turn, gives rise to double strand breaks during the second round of DNA synthesis that then interfere with the replication cycle and result in apoptosis. This theory has been supported by experimental data through the use of MGMT and MMR knockout cell lines [97], human lymphocytes [98] and CHO cell lines [96].

In the rat AOM model however, the 6-8h post AOM time frame in which the peak apoptotic response is reached is deemed to short for apoptosis to be initiated via this failed repair and replication pathway. Considering the cell cycle time in rat distal colon takes more than 48h [173], it may well be the case that this popular theory does not translate completely from an *in vitro* setting into the colonic epithelial environment in an animal model.

Hence, there was a need to measure and compare these types of host responses in the animal model. In particular, it is important to understand when and how rapidly O^6medG DNA adducts form in rat colon in relation to the apoptotic response and also if the rates of cell proliferation change after an insult of AOM. To explore this area and help us better understand the interplay between these responses several parameters, including adduct formation, apoptosis and cell proliferation will be investigated using the rat-AOM model.

Firstly, a 48h time course of apoptosis will be measured to firstly, ensure that the peak apoptotic rate is confirmed to be at the 6-8h time frame and secondly, that no late second wave is observed. The pattern of O^6medG will then be measured

over the same time course to establish where and at what time these adducts appear in colonic epithelium. Finally, cell proliferation rates will be measured to determine if any change in cell cycle rates during this time period occur.

This established time course displaying the level of O^6medG, apoptosis and proliferation is beneficial as it will provide an insight into the relationship between adduct formation and removal in colonic epithelial cells. This insight will allow us to further explore the hypotheses regarding the role O^6medG plays in the initiation of apoptosis as well as providing a basis from which we can explore the potential dietary agents may have in regulating these host responses.

4.1.3. Study design

120 male Sprague Dawley rats at 28 days old (Animal Resources Centre, Canning Vale, Western Australia) were used in this study. Upon their arrival they were housed in a temperature and humidity controlled facility with a daily light/dark photoperiod of 12h. Rats were separated into groups of 4 and housed in cages with raised grid floors to help prevent coprophagy and consumption of bedding materials. Rats were acclimatised for a period of one week during which time they were fed a standard rat chow diet.

Upon the commencement of the experiment, all rats were fed a modified version of the AIN-93 diet [165]. This standard control diet contained a fat/carbohydrate/protein ratio of 20:50:20% respectively. Carbohydrates were added to the diet in the form of 60% cornstarch and 40% sucrose. Casein was used as the protein source and 5% fibre was given as α- cellulose. Sunflower oil with a ratio of 20:70:10 monounsaturated, polyunsaturated and saturated fatty acids was used as the 20% fat source in the diet (refer to table 1 for detailed ingredient list). Diet was made in bulk prior to the experiment and stored at -20°C. Fresh diet was provided daily in pellet form and fed to the rats *ad libitum* for a period of 3 weeks. Fresh drinking water was also provided daily to rats.

At the end of the third week rats were separated into groups of 12 and given a single intraperitoneal injection of the colon specific carcinogen AOM at a dose

of 10mg/kg body weight in the abdomen. One group of 12 rats were given the equivalent volume of saline and were used as the control group. All injections were given as close to 9am as possible to minimise any circadian variability.

Groups of rats were then killed by CO_2 asphyxiation and cervical dislocation at one of 11 time points following AOM administration beginning at 1h and concluding at 48h (see timeline below). The saline treated control rats were killed immediately after the injection (0h). The timeline of this treatment period is summarised below in figure 20.

Figure 20: Time course study time line

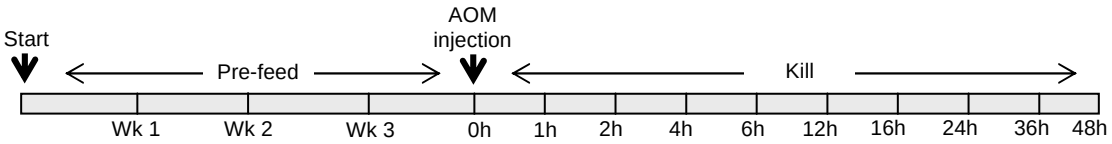

Following the asphyxiation of rats, the entire small intestine and colon of each animal was resected. 2cm sections of both the proximal and distal colon were fixed in formalin to retain the histological morphology of the colonic crypts, while any remaining tissue was snap frozen in liquid nitrogen and stored at -80°C,

Following 12h of formalin fixation, pieces of colonic tissue were cut into smaller sections placed into cassettes, transferred to 70% alcohol and processed in a series of increasing alcohol gradients, xylene and wax overnight (see appendix B). These pieces were then embedded in paraffin wax blocks for long term storage. Using a microtome, 4µm sections were cut and fixed to poly-L-lysine coated slides. Separate colonic sections were cut from each individual rat for each of the histological assays required including apoptosis, O^6medG and cell proliferation.

4.1.4. Results

4.1.4.1. Rat weights

Sprague Dawley rats in total had an average weight of 286.06g, gaining an average of 198.3g over the 3 week feeding period (see figure 21). Though all rats were on the same control diet there was a weight difference between some groups. The largest weight difference was a total of 47g or 15% between group 16h (311.83g) and 36h (264.25g). However, as this was not a dietary intervention study and AOM injections were administered depending on individual bodyweights, the weight difference was considered to be irrelevant to the outcome of the final endpoints.

Figure 21: Rat weights

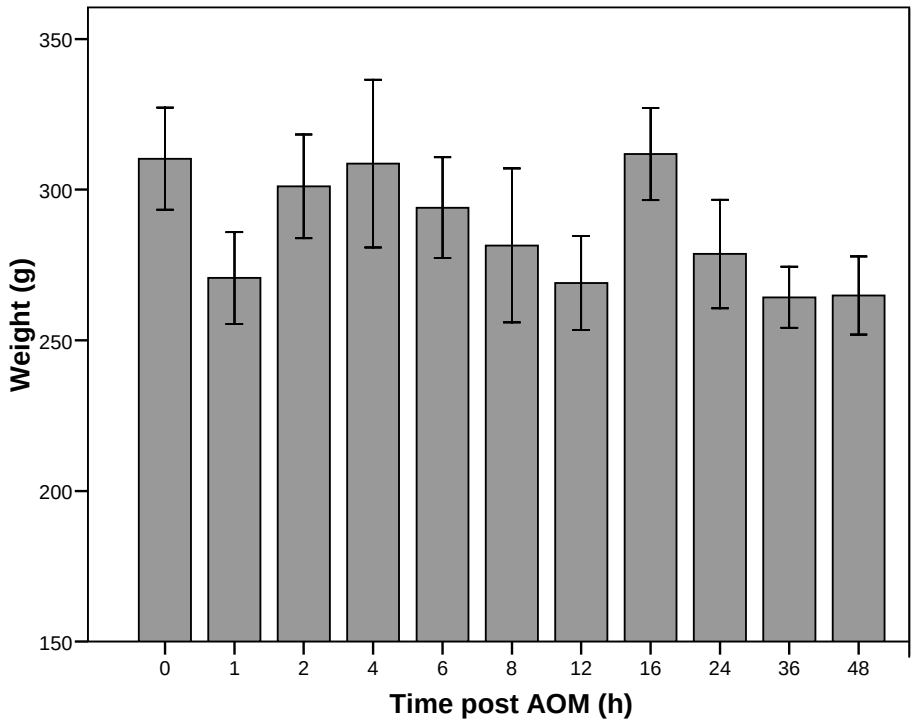

Rat weights grouped according to the time of kill (h) post AOM injection. Final weights were recorded prior to AOM administration. Data are means ± SEM for 132 rats (n=12 rats per group). No significance differences were observed between any groups (ANOVA, Tukey).

4.1.4.2. Time course of apoptosis

In response to the administration of AOM, apoptosis rates were measured in the distal colon over a 48h time period. The AARGC over this time period is displayed in figure 22. Few apoptotic cells were observed in control rats administered with saline (0h time point). Similarly, at 1h and 2h after AOM administration, apoptotic cells were rarely observed within the distal colonic crypts. At 2h however, the number of apoptotic cells in the colonic crypt increased, reaching a maximum level between 6 and 8h of 3.06 ± 0.21 (SEM) and 3.18 ± 0.19 (SEM) respectively. These time points were significantly different from the control group with $p<0.0001$. Following the 6-8h peak, apoptosis levels declined considerably, reaching a level of 1.14 ± 0.19 (SEM) at 12h. Levels then continued to decline gradually, with the exception of a slight increase at 24h of 1.35 ±0.12 (SEM), however this was not significant from surrounding time points and therefore a 'second wave' of apoptosis was not supported from this data.

Figure 22: Number of apoptotic cells per crypt over 48h following an insult of AOM

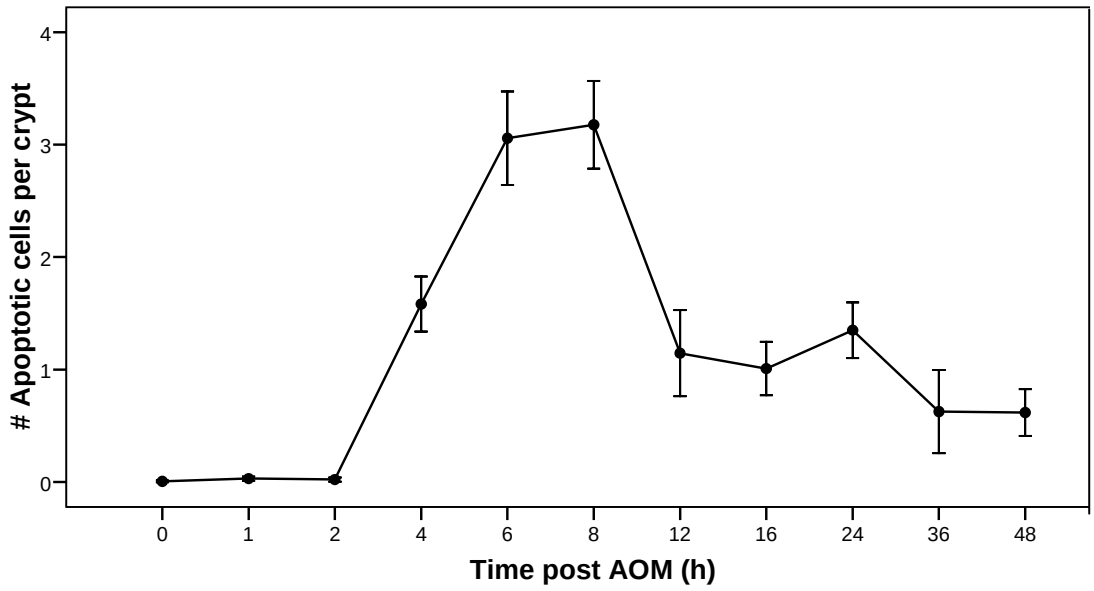

Apoptosis counts over a time course of 48h. Number of apoptotic cells per crypt reaches a maximum at 6 through to 8h. Data are means ± SEM for 132 rats (n=12 rats per group).

4.1.4.3. Time course of crypt cellularity

For the initial 6h post AOM injection the mean cellularity of the distal colonic crypt remained relatively unchanged at an average of 35.44 ± 0.32 (SEM) cells across the first 5 time points as shown in figure 23. At 8h the number of cells along the length of a crypt decreased to the 34.16 ± 0.43 (SEM) and plateaued then out to 16h at which the lowest crypt height of 33.97 ± 0.24 (SEM) was recorded. During the following 20 hour time period an increase in crypt cellularity was recorded until the 48h mark at which the number of cells per crypt returned to resemble numbers observed during the initial time points, 35.08 ± 0.76 (SEM).

Figure 23: Crypt cellularity over 48h following an insult of AOM

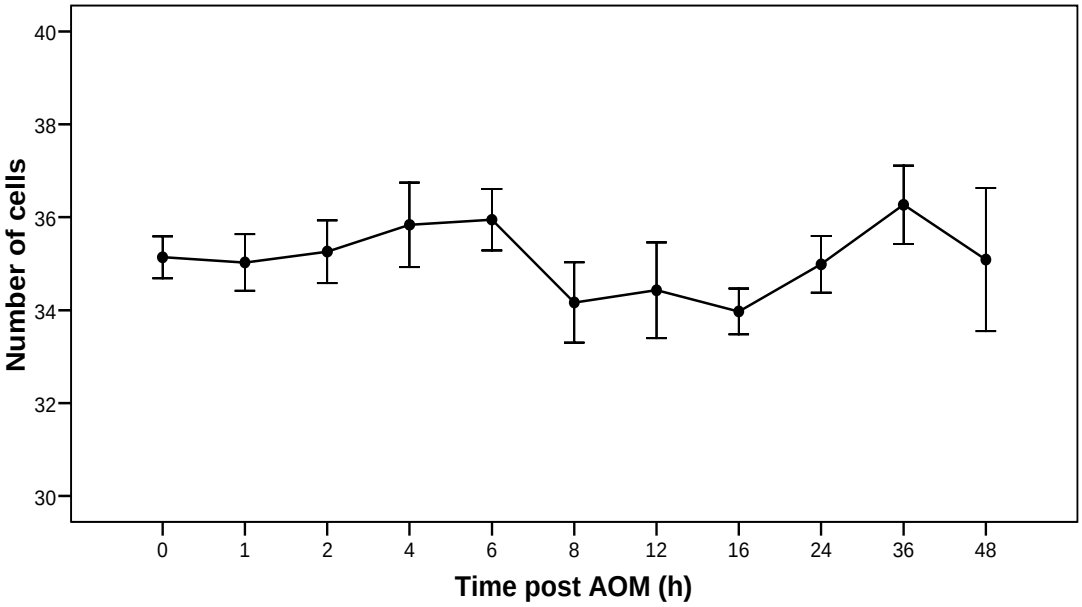

No significant difference was found between crypt cellularity between any time points. Data are means ± SEM for 132 rats (n=12 rats per group).

4.1.4.4. Apoptotic Index (apoptosis / crypt cellularity*100)

Figure 24 displays the apoptotic index over the 48h time course. When the crypt cellularity is taken into account for each time point and a percentage of apoptotic cells per crypt is calculated, the general pattern of the AARGC remains similar to that represented by the raw apoptotic data. This is expected as the cellularity of the crypts across the time course did not change significantly. At the 8h peak, the mean percentage of cells undergoing apoptosis in the distal colonic crypt was a maximum of 9.39% ± 0.55 (SEM).

Figure 24: Apoptotic index over 48h following an insult of AOM

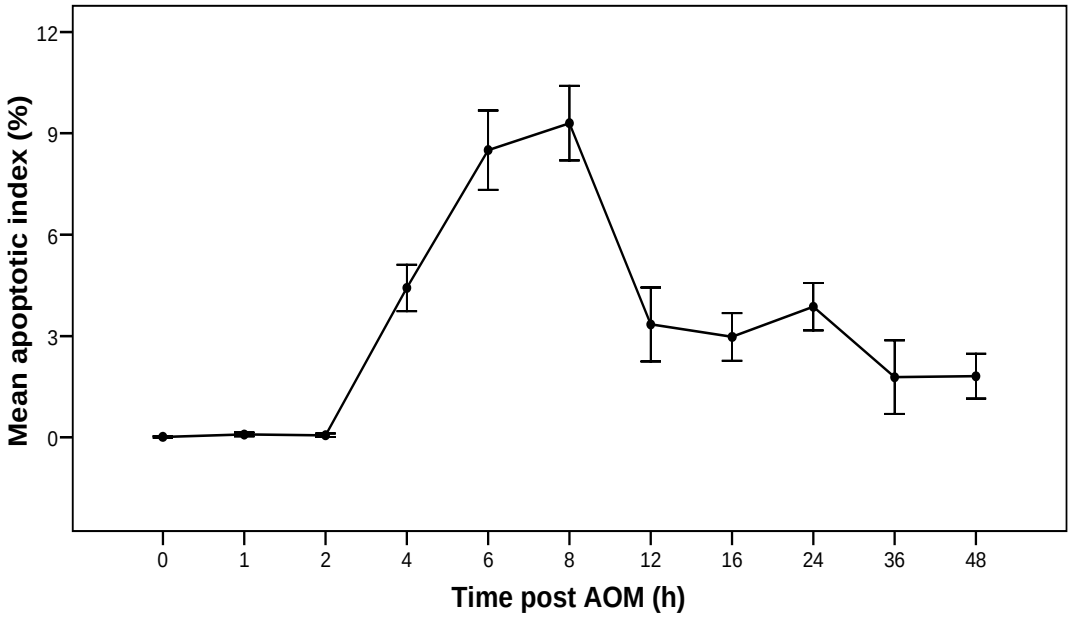

Apoptotic Index represents the percentage of cells within a colonic crypt that are going through apoptosis. Data are means ± SEM for 132 rats (n=12 rats per group).

4.1.4.5. Confirmation of apoptosis using TUNEL assay

The observation of apoptotic cells was confirmed using the TUNEL method of immunostaining. Distal colonic sections from rats killed at four significant time points, 6, 8, 24 and 48h were stained, counted and compared to values obtained when using the haematoxylin assay (see table 2). In all four groups the TUNEL count for apoptosis was slightly higher than that given when using the haematoxylin method. This difference in positive cells however, was comparable for each time point with the TUNEL assay giving a mean increase of 1.03 ± 0.28 (SD) for the number of positive cells across all four time points measured.

Table 2: Apoptosis counts per crypt

Time (h)	TUNEL	Haematoxylin	n
6	4.05 ± 0.4	3.04 ± 0.2	9
8	4.16 ± 0.3	3.13 ± 0.2	12
24	2.7 ± 0.4	1.3 ± 0.1	10
48	1.2 ± 0.1	0.5 ± 0.1	10

All data expressed as means ± SEM for n=41 rats.

Figure 25: Comparison of TUNEL Vs Haematoxylin apoptotic counts

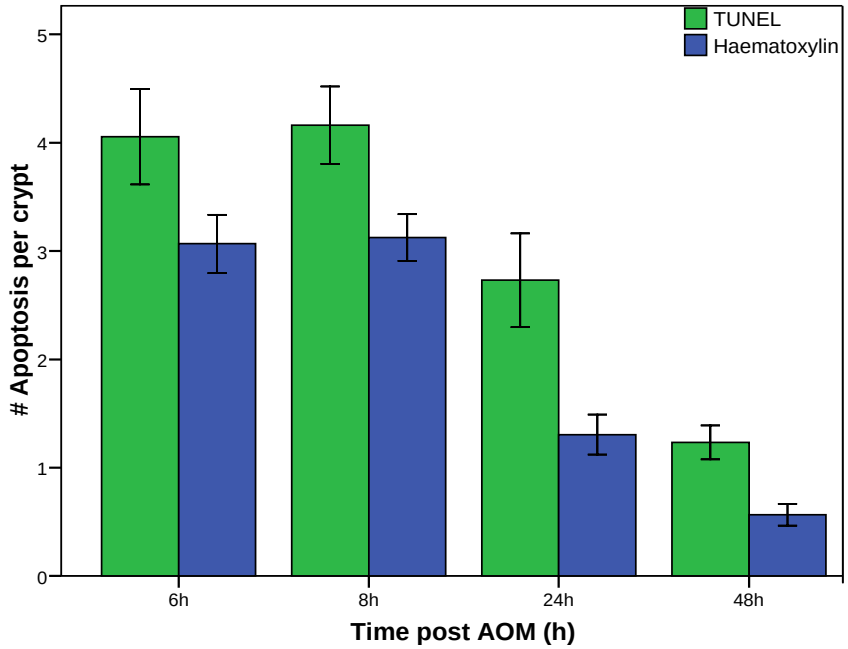

Apoptosis counts over 4 time points counted using TUNEL and Haematoxylin methods. Data are means ± SEM for 41 rats. The differences between time points were retained using either method of staining though TUNEL gave consistently higher counts.

Figure 26: Scatter plot of TUNEL Vs Haematoxylin apoptotic counts

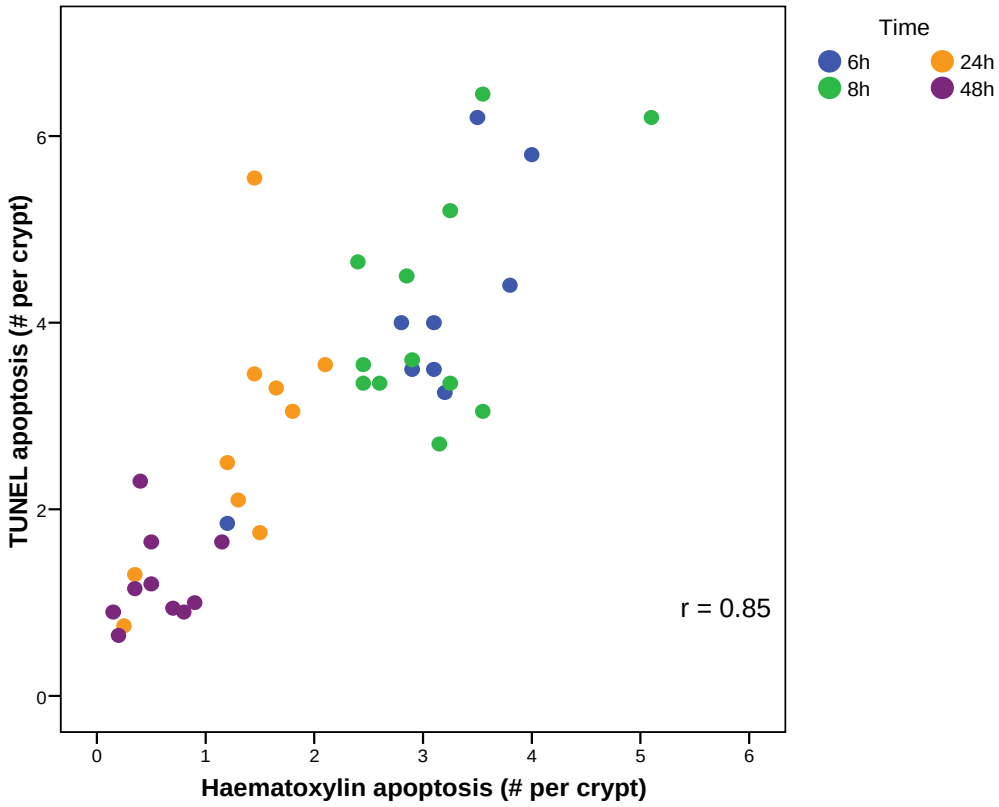

Scatter of apoptosis counts (haemotoxylin method vs TUNEL method) defined by time point (6,8,24,48h) . Pearsons 2-tailed correlation = 0.850. Correlation is significant at 0.01 level.

4.1.4.6. Time course of cell proliferation

Positive cells identified by the presence ki-67 nuclear proliferating antigen appeared brown in colour in contrast to the blue staining negative cells. Counted by eye, the mean number of actively proliferating cells per crypt column was 8.99 ± 0.69 (SEM) at a base line level (0h) as shown in figure 27. Following AOM administration, this number declined slightly until 6h post AOM at which point the number of actively proliferating cells significantly reduced to 6.15 ± 0.48 (SEM) compared to the 0h control ($p = 0.02$). The proliferative rate then increased slightly at 24h and continued to steadily increase at 36h and 48h with the proliferation rate reaching 10.67 ± 0.61 and 11.83 ± 0.58 (SEM) respectively. At 48h the increase of proliferating cells was significantly different to the base line control at 0h ($p = 0.01$).

Figure 27: Number of proliferating cells per crypt over 48h following an insult of AOM

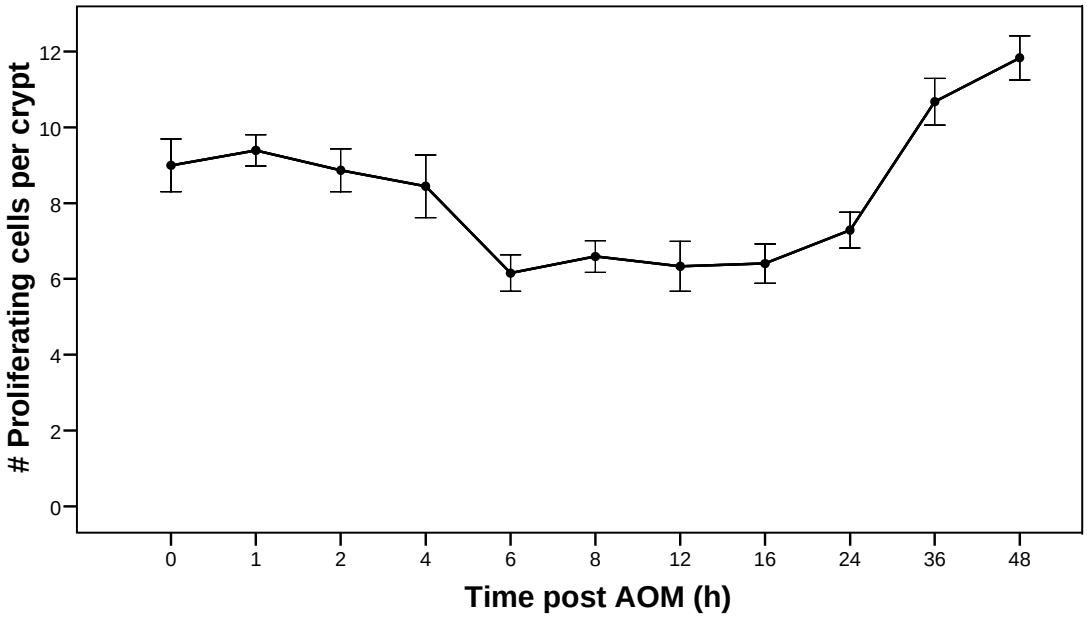

Data displays number of proliferating cells per crypt over 48h. At 6h proliferation rates significantly dropped (p=0.02) compared to baseline levels. Data are means ± SEM for 132 rats (n=12 rats per group).

4.1.4.7. Proliferative Index (cell proliferation / crypt cellularity*100)

When the crypt cellularity is taken into account for each time point and the proliferative index is calculated, the pattern of proliferation does not differ from that shown in the raw data. The percentage of cells actively undergoing proliferation at the baseline level (0h) was measured at 26.16% ± 1.93 (SEM). Like seen in the raw data, the percentage drops significantly at 6h post AOM down to 17.97% ± 1.31 (SEM) and levels out with values of 19.16, 19.11 and 18.26% at 8, 12 and 16h respectively (see figure 28). The significant increase in the percent of actively proliferating cells per crypt as seen with the raw data is also replicated with this percentage reaching 30.70% ± 1.71 and 34.66% ± 1.57 (SEM) at 36 and 48h post AOM.

Figure 28: Proliferative index over 48h following an insult of AOM

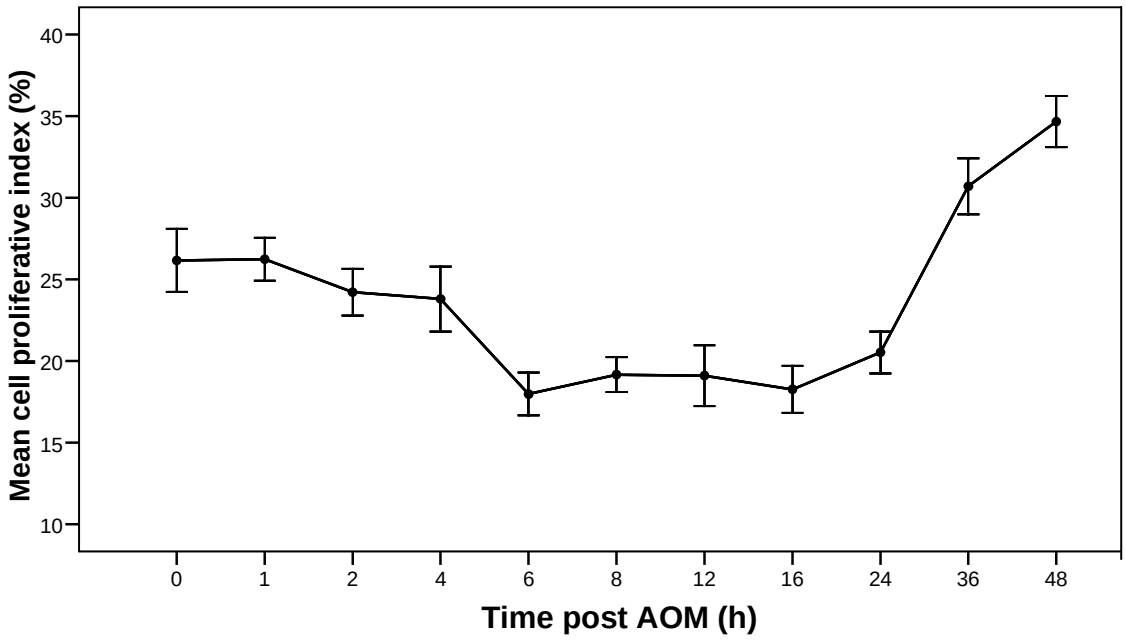

Proliferative Index represents the percent of proliferating cells within a colonic crypt. Data are means ± SEM for 132 rats (n=12 rats per group).

4.1.4.8. Time course of O^6medG DNA adduct formation

O^6medG DNA adducts were not observed in the control rats administered with saline as seen in figure 29A. This negative stain was still quantified using the image analysis system and this baseline RoB ratio was subtracted from all other AOM treated time point groups to eliminate as much background noise as possible.

Figure 29: Images of O^6medG negative and positive staining in rat colonic crypt using the immunochemical assay.

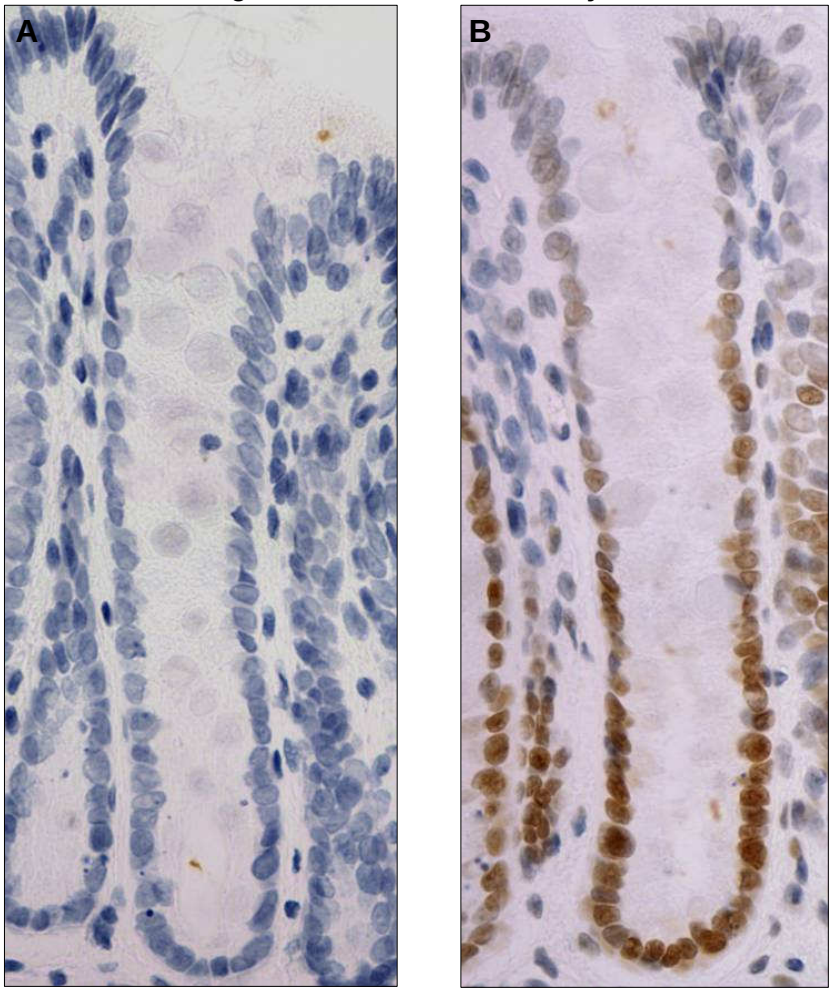

Saline treated control crypt (A) stained negative for O^6medG and an AOM treated (4h) colonic crypt showing positive staining for O^6medG (B).

O^6medG DNA adducts first appeared in the colonic epithelium at 2h post AOM insult measuring 5.58 ± 0.87 (SEM). Levels of O^6medG continued to increase from this point (a stained crypt at 4hpost AOM is pictured in figure 29B), reaching a maximum at 6h post AOM of 11.56 ± 1.72 (SEM). From this point O^6medG levels steadily declined. There was a slight rise in levels at 24h post

AOM, however this increase was not significant and the later 36 and 48h time points continued with the downward trend. At 48h the O^6medG levels of 1.76 ± 0.51 (SEM) at were close to being back at baseline (0h) levels (see figure 30).

Figure 30: Total O^6medG adduct load over 48h following an insult of AOM

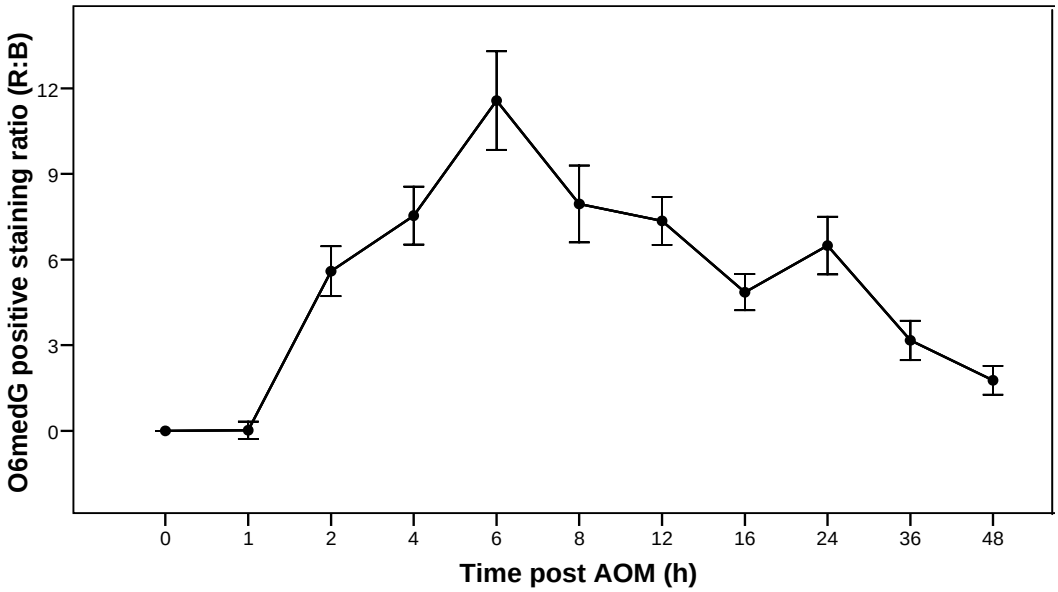

O^6medG formation was first noted at 2h post AOM and peaked at 6h post AOM. From 8h onwards levels steadily declined back towards baseline levels. Data are means ± SEM for 132 rats (n=12 rats per group).

The distribution of O^6medG along the length of the stained colonic crypts varied as the time increased following the AOM injection. The first signs of positive staining at 2h and 4h post AOM were located predominantly in the bottom third of crypts. At 6h the majority of epithelial nuclei along the colonic crypts were positively stained and the intensity of stain was at its highest. At 8h and 12h the nuclei stained strongest for the presence of O^6medG were located at cell positions 7-11 and 14-18 respectively, indicating and upward shift of cells stained positive for O^6medG. A more uniform staining pattern along the crypt was observed at the following 16 and 24h time points, while the final groups at 36 and 48h post AOM displayed a significant drop in the intensity of staining, especially in the lower compartment of the crypt. The change in O^6medG levels along the crypt length is shown in the following section 4.1.4.9 by individual cell position in figure 31A and in crypt thirds in figure 32A. These are also accompanied by distribution data for apoptosis (B) and cell proliferation (C).

4.1.4.9. The distribution of host responses along the colonic crypt

Figure 31A: *O*^{6}medG distribution along the colonic crypt length at different time points

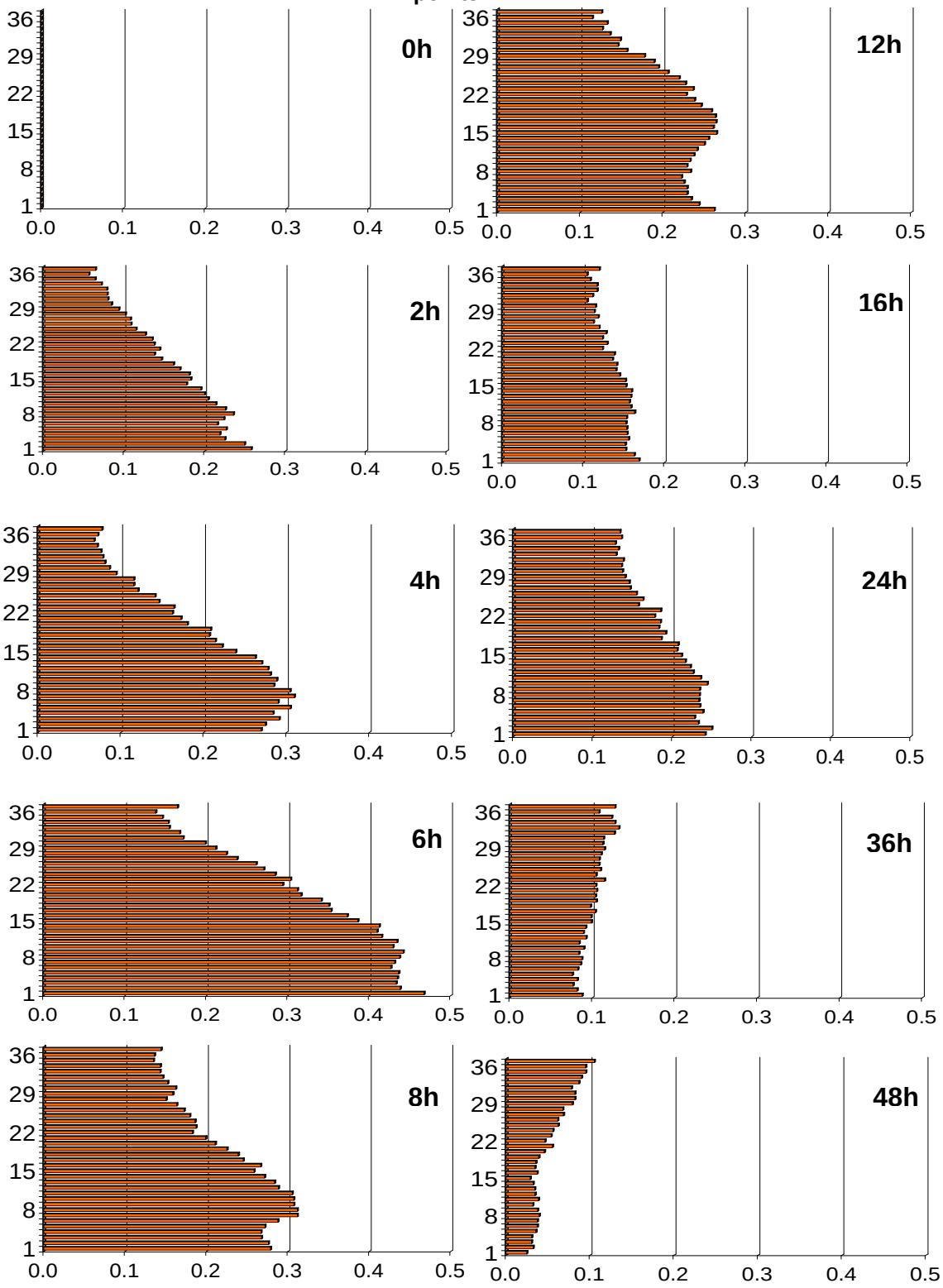

Each graph represents a group (h killed after AOM injection). x-axis = level of O^{6}medG positive staining (RoB ratio), y-axis = cell position along crypt length, from base (#1) to surface (#37). Cell position data represent means for 12 rats per group and means across 20 crypts per rat.

Figure 31B: Apoptotic distribution along the colonic crypt length at different time points

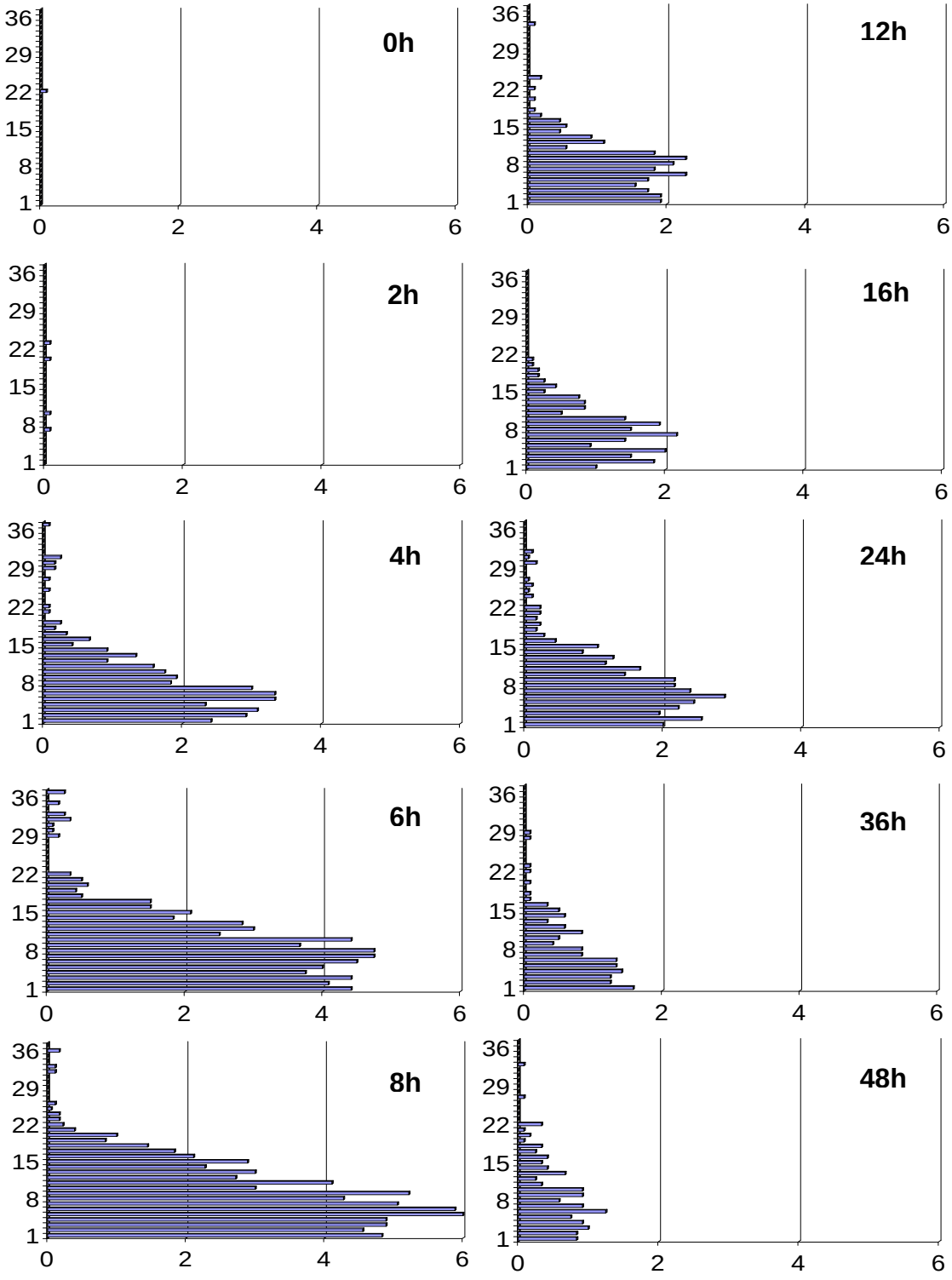

Each graph represents a group at a different time point (h killed after AOM injection).
x-axis = mean number of apoptotic cells per rat, y-axis = cell position along crypt length, from base (#1) to surface (#37). Cell position data represent mean number of apoptotic cells per rat, n=12, 20 crypts counted per rat.

Figure 31C: Distribution of proliferative cells along the colonic crypt length at different time points

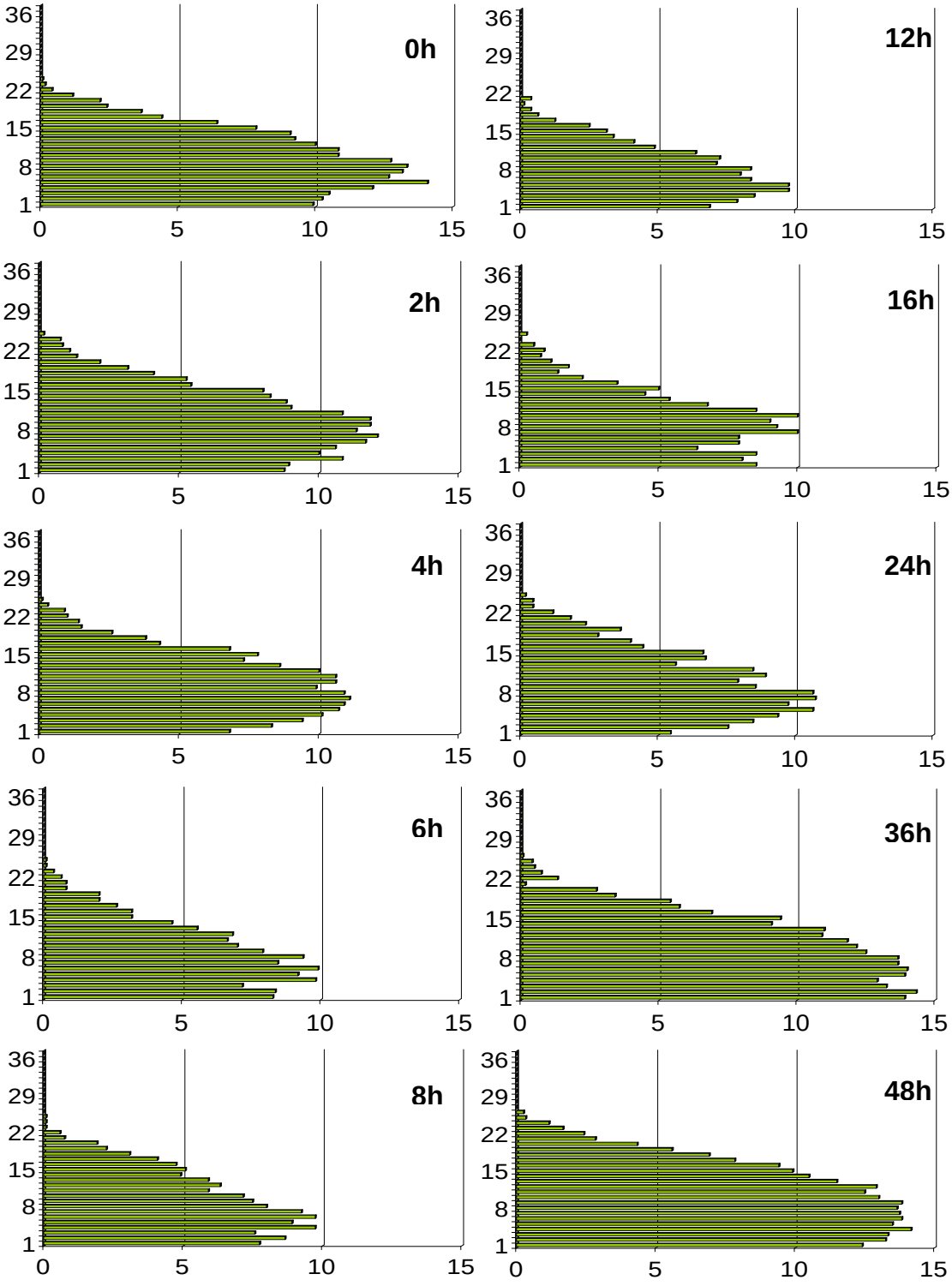

Each graph represents a group at a different time point (h killed after AOM injection).
x-axis = mean number of proliferative cells per rat, y-axis = cell position along crypt length, from base (#1) to surface (#37). Cell position data represent mean number of proliferating cells (as stained by ki-67) per rat, n=12, 20 crypts counted per rat.

The following distribution data (figure 32A-C) has been summarised to show the level of each of the three host responses, O^6medG, apoptosis and cell proliferation when divided into three separate compartments of a colonic crypt. The colonic crypt is lined with epithelial cells that take on different properties and functions depending on where in the crypt they reside. It is well known that the lower third of a colonic crypt is a 'proliferative' zone where the majority of the growth fraction is represented and as these cells move upwards into the middle and upper compartments they become increasingly differentiated and mature. This data is therefore valuable in determining in which zone each of the three host responses exert their maximum effect.

As shown below in figure 32A.1, the individual time points for O^6medG distribution across the three compartments compliments the distribution by individual cellular position as shown in figure 31A. A higher level of O^6medG is present in the lower zone for the 2, 4, 6 and 8h time points, while the 36 and 48h time points see a reduction of O^6medG levels in the lower compartment when compared to the upper compartment.

Figure 32A.1: Change in O^6medG over time by crypt compartment

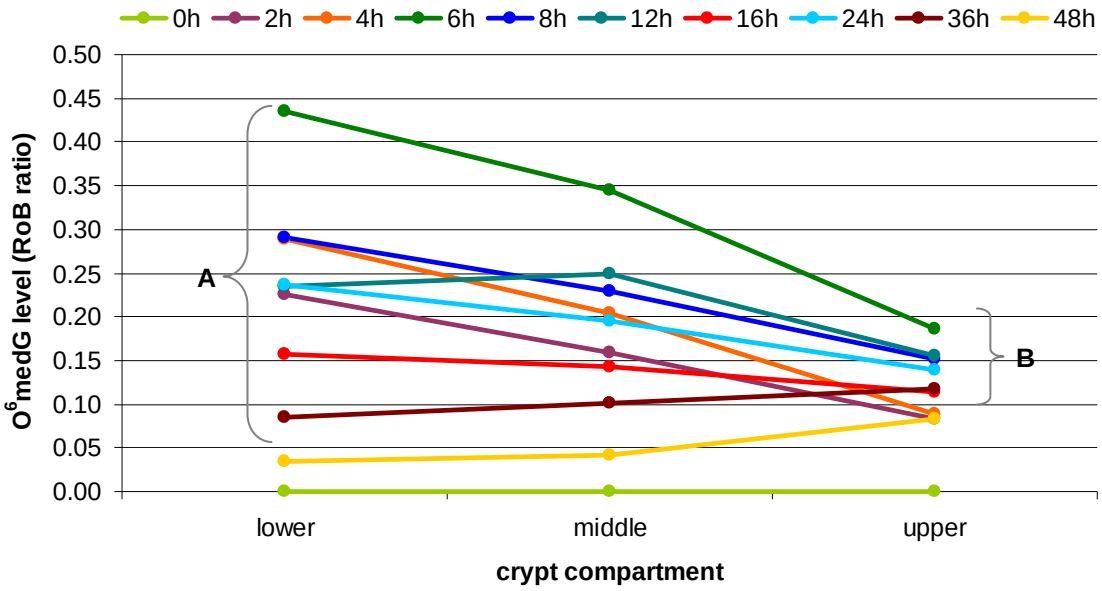

The graph above displays the mean O^6medG level per crypt for each of the 3 compartments of a colonic crypt. 'Lower' represents the mean level for cell positions 1-12, 'middle' represents the mean level for cell positions 13-24 and 'upper' represents the mean level for cell positions 25-37. The F-ratio (a measure used for determining the difference between two sets of variance) for upper means (A) versus lower means (B) is 10.57 (8,8 DoF) and is significantly different at $p<0.01$.

Figure 32A.2 represents the mean level of O^6medG when separated into each of the three crypt compartments over the 48h time period. There is a clear trend which sees a pattern of O^6medG in the lower and middle compartment decline over time. However, there was little difference in the O^6medG level in the upper crypt compartment over time.

Figure 32A.2: Trend of O^6medG levels represented by crypt compartment over

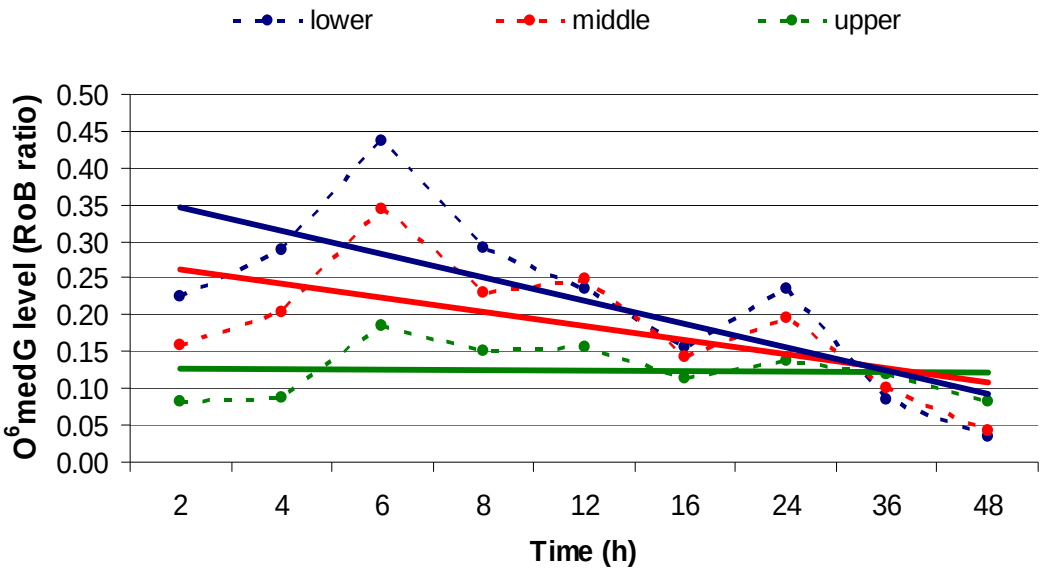

The broken lines represent the mean O^6medG load per crypt for each of the 3 compartments of a colonic crypt over time. This data is accompanied by solid trend lines for each compartment.

Figure 32B.1 displays the total mean number of apoptotic cells for each time point when separated into each of the three crypt compartments, while figure 32.B.2 shows the trend of this response in each of the crypt compartments over the 48h time period. This is repeated in figure 32C.1 and 2 but for the mean number of proliferating cells per crypt.

The distribution of both the apoptotic response and actively proliferating cells is clearly primarily located in the lower compartment of crypts within cells 1 through to 12. These responses also take place in cells located in the middle compartment but to a lesser degree, while the upper compartment containing mature, differentiated epithelial cells remains largely unaffected by these host responses.

Figure 32B.1: Change in the apoptotic response over time by crypt compartment

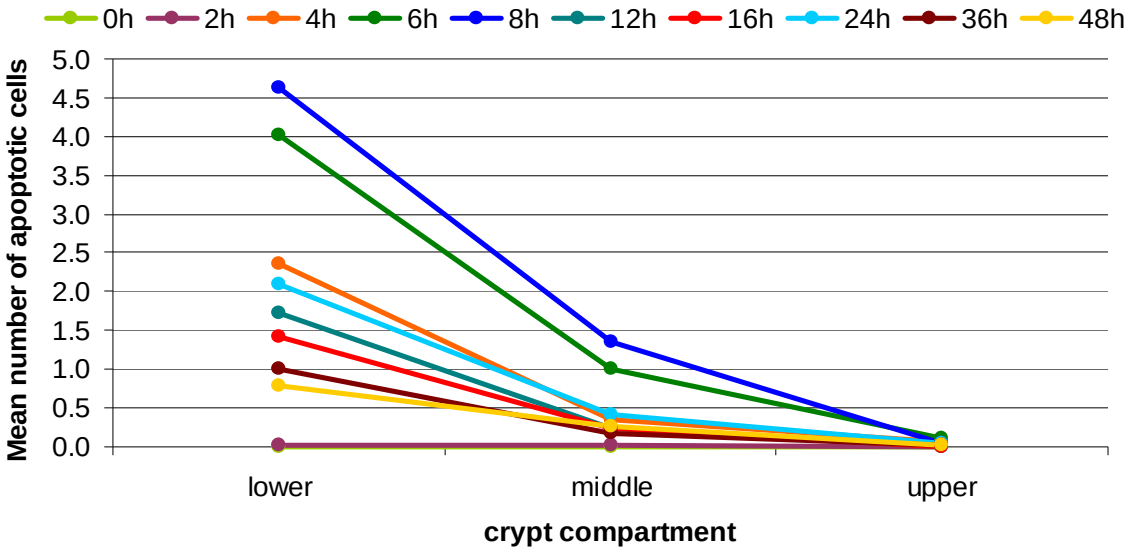

The graph above displays the mean number of apoptotic cells per crypt for each of the 3 compartments of a colonic crypt. 'Lower' represents the mean count for cell positions 1-12, 'middle' represents the mean count for cell positions 13-24 and 'upper' represents the mean count for cell positions 25-37.

Figure 32B.2: Trend of apoptosis represented by crypt compartment over 48h

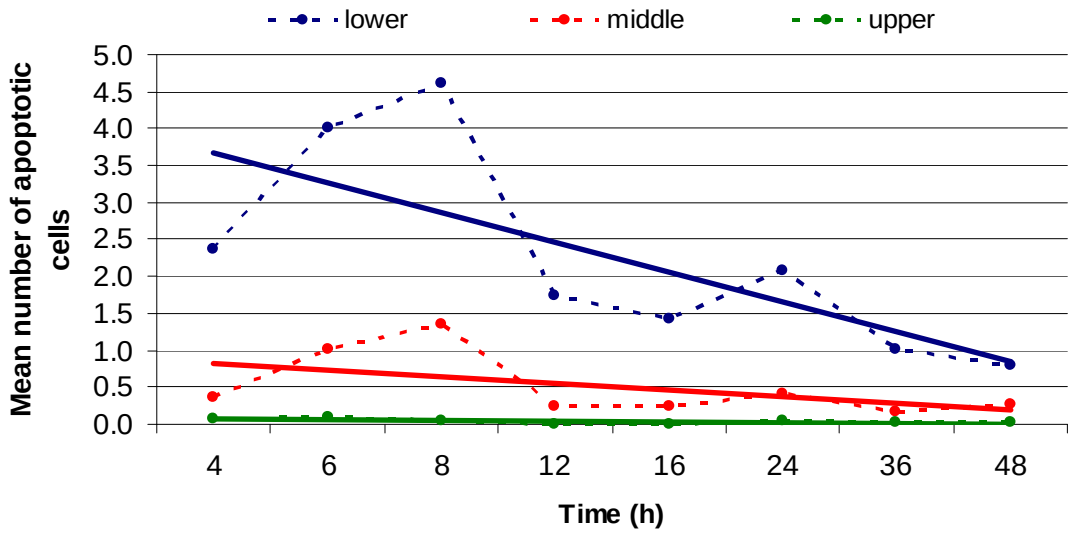

The broken lines represent the mean number of apoptotic cells per crypt for each of the 3 compartments of a colonic crypt over time. This data is accompanied by solid trend lines for each compartment.

Figure 32C.1: Change in cell proliferation over time by crypt compartment

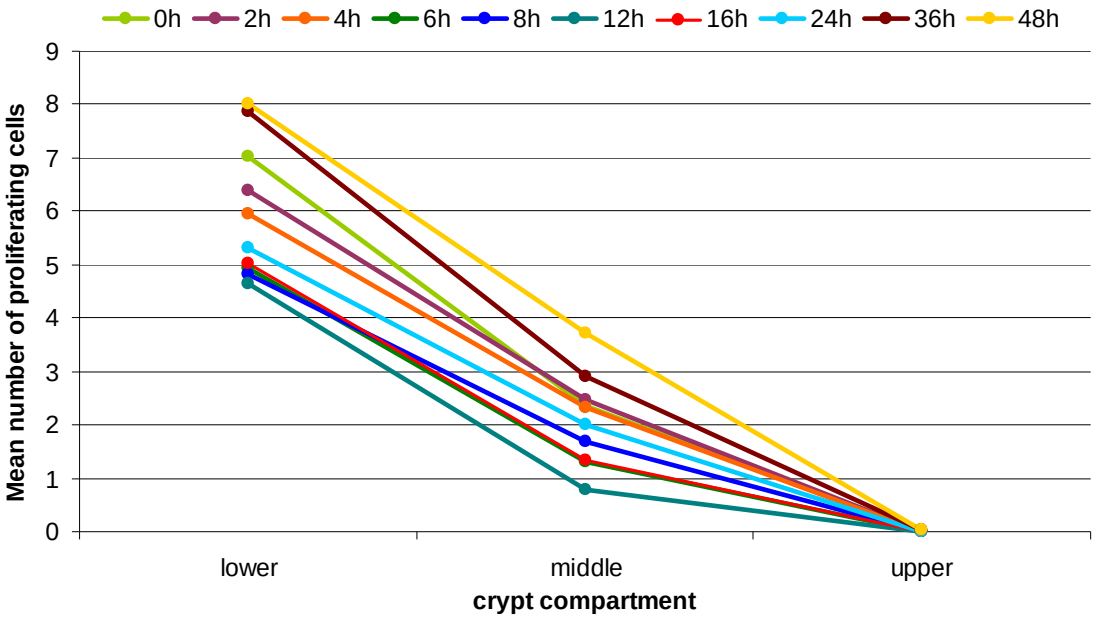

The graph above displays the mean number of proliferating cells per crypt for each of the 3 compartments of a colonic crypt. 'Lower' represents the mean count for cell positions 1-12, 'middle' represents the mean count for cell positions 13-24 and 'upper' represents the mean count for cell positions 25-37.

Figure 32C.2:Trend of cell proliferation represented by crypt compartment over 48h

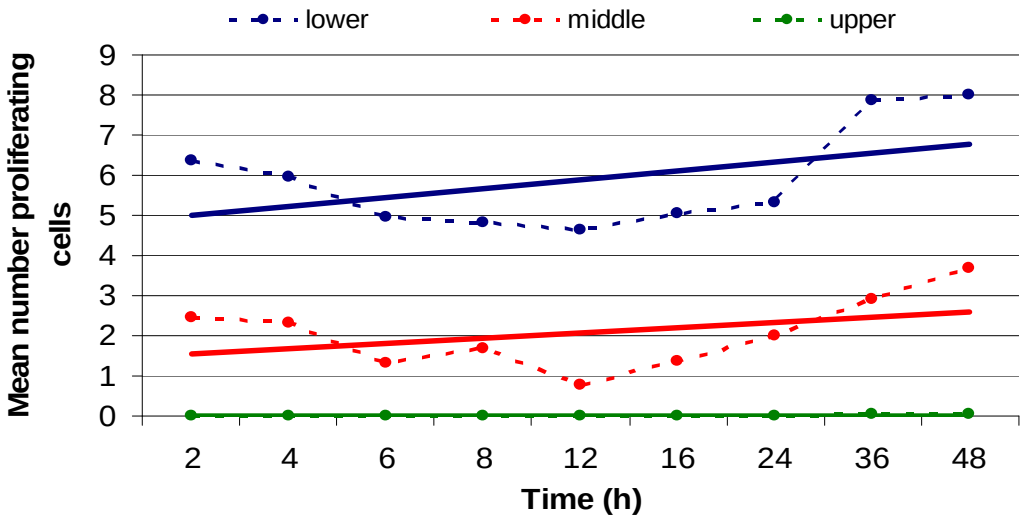

The broken lines represent the mean number of proliferating cells per crypt for each of the 3 compartments of a colonic crypt over time. This data is accompanied by solid trend lines for each compartment.

4.1.4.10. Data summary

Figure 33 and table 3 summarise the results for all three endpoints; apoptosis, O^6medG and cell proliferation over the 48h time period. As shown below, both the onset of apoptosis and O^6medG formation occurred rapidly following an insult of the alkylating agent AOM, they then both continued to peak at approximately 6 and 8h and declined from this point onwards. Cell proliferation on the other hand significantly decreased 6h post AOM and plateaued from this point onwards until the 24h mark at which time the number of actively proliferating cells significantly increased.

Figure 33: Apoptosis, O^6medG and cell proliferation levels over 48h following an insult of AOM

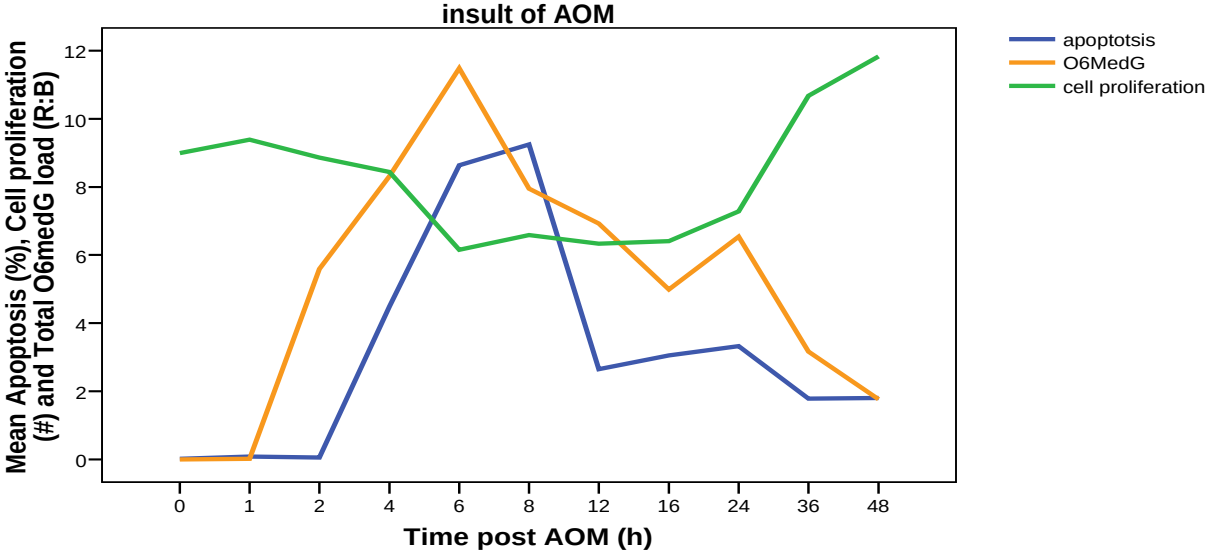

Apoptotic counts represented as % of apoptotic cells per crypt, cell proliferation represented as # of proliferating cells per crypt and O^6medG represented as total O^6medG adduct load per crypt.

Table 3: Summary of acute homeostatic responses in colonic epithelium over time in response an insult of alkylating agent

Time point (h)	Apoptosis (# per crypt)	Cell proliferation (# per crypt)	O^6medG DNA adduct (RoB staining ratio)
0	0.01 ± 0.01	8.99 ± 0.69	0.00 ± 0.00
1	0.02 ± 0.01	9.39 ± 0.42	0.01 ± 0.31
2	0.02 ± 0.01	8.87 ± 0.57	5.58 ± 0.87 [a]
4	1.58 ± 0.12 [a]	8.44 ± 0.83	7.53 ± 1.01 [a]
6	3.06 ± 0.21 [a]	6.16 ± 0.48 [a]	11.56 ± 1.72 [a]
8	3.18 ± 0.19 [a]	6.59 ± 0.42	7.94 ± 1.34 [a]
12	1.15 ± 0.19 [a]	6.33 ± 0.66	7.35 ± 0.84 [a]
16	1.01 ± 0.12 [a]	6.41 ± 0.52	4.85 ± 0.63 [a]
24	1.35 ± 0.12 [a]	7.28 ± 0.47	6.48 ± 1.01 [a]
36	0.62 ± 0.18	10.67 ± 0.62	3.16 ± 0.69
48	0.62 ± .11	11.83 ± 0.58 [a]	1.76 ± 0.51

Time point groups represent time of kill after AOM administration, with 0h being control saline group. All data expressed as means ± SEM. [a] P< 0.05, compared with 0h saline control group (ANOVA, Tukey)

4.1.5. Discussion

This time course study allowed the newly developed O^6medG immunohistochemical assay to be tested in detailed. Distal colon sections of rats killed at different time points post AOM were successfully stained for the presence of the O^6medG adduct. A clear pattern of O^6medG formation and removal was observed over the 48h time period reaffirming both the specificity and sensitivity of this assay. Furthermore, this pattern of staining as seen by eye was reflected in the final image analysis data.

As expected, no colonic O^6medG adducts were detected in the distal colon of saline treated control rats. Similarly, O^6medG adducts were not detected in the colon of animals killed 1h after AOM. The first detectable sign of O^6medG adducts was observed in animals killed 2h post AOM administration. The degree of O^6medG damage at this stage was minimal and was refined to the nuclei of epithelial cells in the lower proliferative compartment of the colonic crypts. From this point onwards the O^6medG load and distribution increased throughout the crypt, peaking at 6h post AOM. O^6medG levels then steadily declined until they were near to base line levels at the final measured time point of 48h. These results are in contrast to those published by Hong *et al* [61], which described an increasing gradient of O^6medG through up until the 12h mark. This may have been the result of the increased dose of AOM used (15mg/kg) in comparison to our 10mg/kg dose or alternatively it may simply be an artefact of different use of immunohistochemical methods and image analysis practices.

In addition to this, the Hong paper also details a more uniform measurement of O^6medG throughout the entire crypt at every time point measured, which again is in contrast to this study in which a varying distribution of O^6medG was recorded at different time points as discussed further on.

The measured AARGC over the 48h time period corresponded well with previous studies that have also measured this response in the distal colon [77]. The onset of apoptosis was first observed 4h post AOM and peaked between 6

and 8h. This response primarily occurred in the lower compartment of colonic crypts, affecting cells in position 1 through to 12. Resembling the pattern of O^6medG, the number of apoptotic cells per crypt also declined towards baseline levels following the 6-8h peak. Though a slight, insignificant increase was measured at 24h post AOM this did not constitute a so called 'second wave' of apoptosis as has previously been observed in the small intestine [174]. This experimental data does not support the suggestion of a later second wave of apoptosis in the colon between 8 and 48h following an insult of AOM.

The use of haematoxylin staining is a valid and widely used method in identifying apoptotic cells in the colon [77, 174-176]. However, to support these apoptotic results the TUNEL assay was carried out on animals at four significant time points post AOM treatment. The apoptotic counts carried out by the TUNEL method correlated well with those using the haematoxylin stain. This reinforces the later assay as a reliable and competent method of measuring the AARGC in the rat colon. Though comparable, the TUNEL apoptotic counts did tend to be slightly higher across all time points. This observation corresponds with other studies [77, 177], supporting the suggestion made by Hu *et al*. that the TUNEL method may be more sensitive in detecting DNA strand breaks before they are translated into the visible morphological effects that eventually occur in the nuclei of cells.

The crypt height measured during the analysis of all endpoints was not significantly affected over the 48h time period. An average reduction in crypt height of approximately one cell was observed at 8, 12 and 16h. This slight reduction may have been due to the increase in the removal of cells via apoptosis at this time. Nevertheless, this difference was not considerable enough to impact the apoptotic counts or proliferative counts when they were calculated as a percentage for each crypt.

The detection of actively proliferating cells was carried out by an immunochemical assay using the ki-67 antibody. Cells staining positive for the presence of this proliferating protein are in either in S phase and also the G_1, M and G_2 phases of the cell cycle [178]. Findings from this time course study show

that the number of actively proliferating cells decreases 6h after an insult of the genotoxin. This lower level of cells within the cell cycle remains steady until the 36h mark post AOM in which the number of actively proliferating cells significantly increase.

Previous studies have demonstrated an acute inhibitory effect of mitosis and DNA synthesis in cells following exposure to a genotoxic agent [179, 180]. Our findings support this concept with a significant decrease in the number of proliferating cells observed 6h post AOM insult.

When the host responses to an insult of AOM were analysed in terms of their distribution along the crypt length, it was apparent that the majority of cells undergoing apoptosis or proliferation were located in the lower crypt third from cell position 1 to 12 and changes in this lower compartment were the principal reason behind changes in total numbers of both of these endpoints overall. The O^6medG load however, at all the time points measured, was readily detectable within both the lower and middle compartment of the colonic crypts, and unlike the apoptotic response was also detected in the upper crypt compartment.

More specifically, unlike the apoptotic response, the distribution of O^6medG along the crypt length changed over the 48h period following AOM administration. This shift in distribution has not been reported in other studies using immunochemistry to measure O^6medG in the colon [61]. From 2 to 8h following the AOM insult, cells with nuclei containing O^6medG were primarily located in the lower and middle crypt compartments. A more uniform distribution was then observed between 12 and 16h, while the later time points of 36 and 48h showed a greater level of O^6medG in cells located within the upper third of the crypt.

A number of reasons may be behind this shift in O^6medG distribution over time. Firstly, it is possible that the shift in distribution along the crypt may represent a natural migration and differentiation of the once actively proliferating colonic cells that were originally exposed to the AOM insult rather than new damage to the more mature surface cells. Cell migration studies suggest that the length of

time taken for a colonic epithelial cell to migrate along the crypt length is approximately 60-72h [173] and while the reduction in cell proliferation rates after an insult of AOM does not necessarily support this rapid growth and push of cells up the colonic crypt, it is still feasible that this shift may be due in part to the natural kinetics of the colonic crypt.

However, we propose an alternative and more plausible explanation behind this shift in O^6medG levels along the crypt length that can be attributed to the apoptotic response. We believe that the change in the distribution of O^6medG levels along the crypt over time is more representative of the change and location of the apoptotic response in the crypt rather than a matter of simply cell kinetics.

Like the apoptotic response, the O^6medG distribution data shows that the change in total levels of O^6medG can be attributed to a change in O^6medG levels in cells located primarily within the lower crypt compartment rather than the upper crypt compartment. This is supported by the fact that the O^6medG levels in cells within the upper crypt compartment remain relatively steady across all time points, while the variation between O^6medG levels in the lower zone between the different time points is extensive. Therefore, we know that the apoptotic response not only closely follows the formation O^6medG, but also occurs in the same lower proliferative compartment in which O^6medG levels are being affected. We therefore propose that O^6medG levels do not necessarily shift upwards along the crypt with cells over time. But rather, that the apoptotic response is a key mechanism for which O^6medG is removed from the lower compartment of the colonic crypt and this reduction of O^6medG from the lower compartment is why a change in O^6medG distribution was observed over time.

One may assume that if this time course study was extended and O^6medG was measured in animals killed 72h post AOM or later, a further and complete reduction of O^6medG levels may be observed due to the removal via apoptosis and also as the result of the complete renewal of epithelial cells in colonic crypts. The completion of such an experiment would be of use in determining the total and comprehensive cycle of O^6medG formation and removal in rat colonic epithelial cells in response to AOM.

In addition to providing information about the critical colonic host responses to AOM, this study allowed us to explore the concept of O^6medG-mediated apoptosis. As discussed in section 4.1.2, the current theory explaining the link between O^6medG and apoptosis has been extensively studied using *in vitro* models. It is proposed that apoptosis is triggered via the MMR pathway due failed repair of the base mispairs caused by O^6medG lesions [95]. This proposed pathway requires the completion of two cell cycles in order for apoptosis to transpire. Doubts were previously held concerning the length of time available for the completion of this pathway in rat colonic epithelial cells. Findings from this time course study support these reservations.

Findings from this *in vivo* study show that there is approximately a 2 hour delay between the formation of O^6medG and the onset of apoptosis over the 48h time course and no second wave. Two rounds of DNA synthesis can not be completed in this 2 hour time frame and therefore this pathway of O^6medG-mediated apoptosis is unlikely in AOM treated rat colonic cells. In addition to this, the cell proliferation data which imply a stalling effect on the cell cycle 6h post AOM administration also add to the doubts of this particular O^6medG-mediated apoptotic pathway occurring *in vivo* with AOM.

The pathway of O^6medG-mediated apoptosis has been extensively tested and studied using *in vitro* models and is well accepted. Therefore, our findings question the ability to relate this data into the rat-AOM *in vivo* model, rather than the proposed pathway itself. It is possible that this pathway as tested *in vitro* can not be entirely translated to an *in vivo* setting. In addition to this, the specific tissue type being tested and the carcinogen treatment used may all respond differently and therefore, it is suggested that any *in vitro* data when applied to an *in vivo* model must be cautiously interpreted.

The close pattern of the O^6medG and apoptotic response in colonic cells suggests interplay between these responses. While these responses may simply be parallel events that are not related to each other, it is also possible that apoptosis may be triggered via a more direct pathway. Given the short time period between O^6medG and apoptosis, it is possible that apoptosis may be initiated by a direct

trigger resulting from the formation of O^6medG. One such pathway has been proposed that still involves the MMR system but operates via a more direct cell signalling pathway. It has been suggested that instead of initiating apoptosis via failed repair and the formation of DSBs, MMR proteins can also act as a general sensor of the O^6medG adduct and play a direct signalling role in initiating apoptosis instead. As reviewed by Kaina *et al* [181], it has been shown that MMR proteins, and the MutSα complex in particular can bind to O^6medG adducts directly and activate ATR/ATRIP signalling. What remains to be shown however, is whether this activation is sufficient to activate the Chk1 and P53 pathway and result in apoptosis.

Therefore, to rule out whether MMR does play any part in the initiation of the AARGC in the colon via either the failed repair or a possible direct signalling pathway, the measurement of the acute host responses in a MMR deficient-AOM rodent model is recommended. In addition to this, the use of a controlled O^6medG regulating agent, such as a repair (MGMT) inhibitor or varied doses of carcinogen can also be used in future *in vivo* studies to test the possibility of more of a direct link between O^6medG and apoptosis.

While, these suggested studies were not able to be completed in the time frame of this research, the potential of an alternative BER-mediated apoptotic pathway was investigated by undertaking a simple acute animal study. This is explained in detail in the following section (4.2).

This time course study has identified the pattern of the important host responses in colonic epithelial cells following an insult of AOM. In particular, the 6h mark post AOM appears to be a noteworthy time point in which all endpoints measured had a significant response. The peak O^6medG load was recorded at the 6h mark while the number of proliferating cells significantly decreased at this time. Furthermore, while the apoptotic response peaked at 8h post AOM, the 6 and 8h time points were not significantly different. Hence, future dietary intervention studies that focus on the regulation of these host responses will be carried out on samples reflecting the significant 6h post AOM time point.

4.2. Methoxyamine study

4.2.1. Aims

This additional study was included to look into possible pathways involving adduct formation that may play a role in the initiation of apoptosis. The aim of this study was to determine whether the onset of apoptosis in the acute AOM rat model is influenced by the BER pathway. In particular, the specific aims are as follows;

1. Administer rats with MX alone and also a combination of AOM and MX at 10mg/kg b.w. and observe any negative physical effects of these chemicals.

2. Count and compare the apoptotic rates at 6h post injection with a standard control AOM group.

4.2.2. Experimental rationale

As previously pointed out, current popular theory suggests that apoptosis is initiated after the failed repair of O^6medG via MMR and the resulting formation of DSBs over two cell cycle periods. Initially it was thought that this pathway of apoptosis initiation in the rat model would not be feasible due to the short time frame in which apoptosis appears after an AOM insult.

At present, observations taken from the time course study suggest that this pathway is even more unlikely. Our findings show that O^6medG first appears in the nuclei of cells 2h post AOM, while apoptosis was first noted 4h post AOM. Therefore, these findings suggest that only a 2h delay between the formation of O^6medG and the initiation of apoptosis exists. As the cell cycle itself takes over 48h in the distal colon [173], the concept of the O^6medG mediated apoptosis pathway that requires the formation of DSB, is not feasible in rat colonic epithelium.

We suggest that the acute apoptotic response to AOM in this *in vivo* model may be triggered by another mechanism. It is possible that O^6medG itself acts as a direct trigger of apoptosis *in vivo*, or alternatively, that acute apoptosis is initiated by other events completely. As the role of the MMR pathway in the late apoptotic response *in vitro* has clearly been demonstrated, it was decided that the role of an alternative repair pathway such as BER in the apoptotic process *in vivo* would be explored in this study.

It is well established that BER is an important pathway that cells initiate to efficiently remove DNA lesions including N3meA, N3meG and N7meG and possibly O^6medG [182]. BER is a multi-protein system that facilitates the recognition and repair of such methylated bases through a number of diverse damage-specific glycosylases [183, 184]. However, regardless of the type of damage or the respective glycosylase used, the excision repair of these incorrect bases always results in the formation of an apurinic/apyrimidinic (AP) site [185]. From this point, the resulting one nucleotide gap is subjected to a series of processes required for the synthesis and ligation of a single-nucleotide DNA, effectively repairing the initial damaged base.

It was hypothesised that the possible initiation of the BER repair pathway, via O^6medG or by other means, may play a role in the acute apoptotic response as observed in the colon of rats. To test this hypothesis a short term study was designed using the chemical methoxyamine (MX).

MX is a chemical that when administered to rats will effectively block the base excision repair pathway. MX interferes with the BER pathway by reacting with the aldehydic carbon 1 atom of an AP site [186, 187]. This stalls the BER process as the next β-elimination step of the dRP lyase mechanism is unable to go ahead. Furthermore, the MX-AP site is also resistant to the enzymatic removal by APE [188] and therefore, the BER pathway is disrupted and the progression of this type of repair is effectively blocked.

The BER mode of recognition and repair will be disabled in the rat using an injection of MX at a dose of 10mg/kg b.w. Doses within this range have been

shown to be safe and effective by Liu *et al.* when tested on nude mice [189]. The acute apoptotic response will be analysed 6h after AOM administration at an equivalent dose of 10mg/kg b.w. Apoptosis rates will be compared to control groups subjected to AOM and MX independently.

If the apoptotic response if significantly reduced or eliminated in the AOM/MX, BER deficient group it can then be concluded that the BER pathway does indeed play a role in the initiation of apoptosis via O^6medG or through other means.

4.2.3. Study design

36 male Sprague Dawley rats at 28 days old were fed on the standard control diet used in the time course study for a period of 2 weeks. Fresh diet as well as fresh drinking water was provided ad libitum on a daily basis. At the end of the second week rats were weighed individually and separated into 3 groups of 12 (see table 4).

Figure 34: MX Study timeline

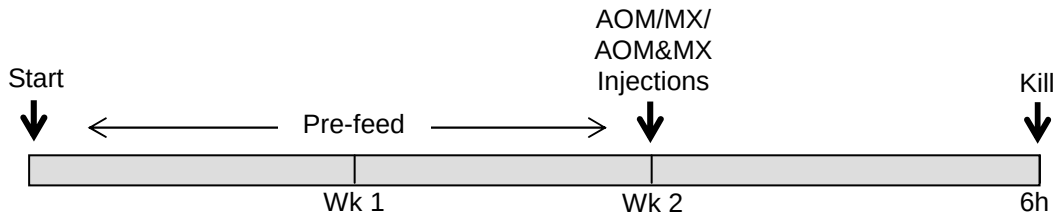

The first group was given a single injection of AOM at 10mg/kg of their body weight. Liu *et al* [182] previously demonstrated that the highest tolerable dose of MX in nude mice was 120mg/kg, while a dose of 2mg/kg was sufficient enough to decrease the number of ARP-reactive AP sites and therefore effectively block BER in these areas. This group also reported that the effect of MX upon AP sites *in vivo* is somewhat lower than that observed *in vitro* and therefore, it was decided that the MX in this pilot study would be administered to the rats at the equivalent dose of AOM at 10mg/kg. Hence, the second group was given a single injection of methoxyamine at 10mg/kg b.w., while the third and final group were given two individual injections of both the AOM and the

MX at 10mg/kg b.w. These injections were given immediately after each other and were all administered as close to 9am to minimise any circadian variability

Table 4: MX Study Groups

Group	Diet	Treatment	Number
1	Control	AOM (10mg/kg b.w.)	12
2	Control	MX (10mg/kg b.w.)	12
3	Control	AOM (10mg/kg b.w.) and MX (10mg/kg b.w.)	12

Six hours following the administration of injections all animals were killed by CO_2 asphyxiation and cervical dislocation. The colon of each animal was resected and a 2cm section of the far distal end was fixed in formalin overnight. Tissue sections were then processed and embedded in paraffin wax ready for histological assessment. 4µm thick wax sections were stained in haematoxylin and counted for apoptosis levels.

4.2.4. Results

4.2.4.1. Apoptosis

Apoptotic data are presented as number of apoptotic cells per crypt in figure 35. The control group injected with AOM alone had the highest mean apoptotic count of 3.89 ± 0.41 (SEM), while the AOM + MX group had a mean count of 2.87 ± 0.34 (SEM). These two groups were not statistically significantly different from each other, though the MX treatment did appear to have some effect on the genotoxicity of the AOM, as the AOM + MX treated group did have fewer apoptotic cells per crypt. Rats injected with MX alone had minimal apoptotic cells observed with a mean count of 0.01 ± 0.01 (SEM), which is comparable to values previously observed in saline injected control groups.

Figure 35: MX Study Apoptosis counts

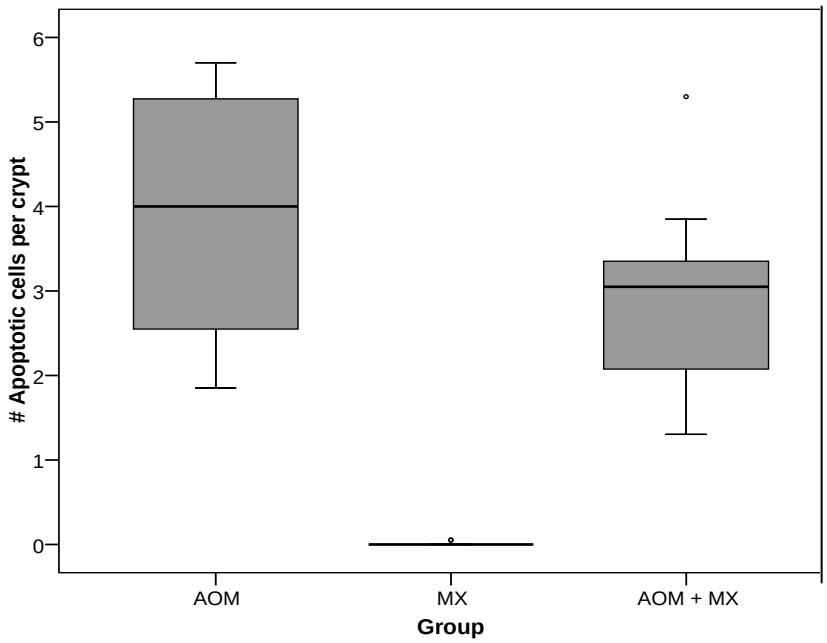

Data represents number of apoptotic cells per crypt. Data are means ± SEM for 36 rats (n=12 rats per group). AOM = Azoxymethane (10mg/kg bw), MX = Methoxyamine (10mg/kg bw), AOM + MX = Azoxymethane and Methoxamine (10mg/kg bw).

Table 5: MX Study Apoptotic counts

Group	Apoptosis (# per crypt)	Crypt cellularity	Apoptosis (% per crypt)
AOM	3.89 ± 0.41	38.43 ± 0.34	10.07 ± 1.05
MX	0.01 ± 0.01 [a]	37.78 ± 0.16	0.03 ± 0.16 [a]
AOM + MX	2.87 ± 0.34	38.01 ± 0.56	7.42 ± 0.82

All data expressed as means ± SEM. [a] P< 0.05, compared with AOM control group (AOM control group Vs AOM + MX group P= 0.07). No difference was observed in crypt cellularity and therefore apoptotic index (%) remained unchanged.

4.2.5. Discussion

This study aimed to look at the effects of the BER blocking chemical, methoxyamine, in the rat-AOM model. Firstly, this study confirms the safety of MX at a dose of 10mg/kg b.w. in the rat when combined with the AOM carcinogen as no detrimental effects were observed either during the time of injection or in the period before the animal kill.

Additionally, the administration of MX alone in the rat did not appear to have any immediate toxic effects on any of the animals as observed from their physical states. Apoptosis levels in the MX group were comparable to those observed in saline injected rats in section 4.1.4.2. This lack of any notable apoptotic response in the colon suggests that the administration of the chemical MX does not have any genotoxic effects on colonic epithelial cells of rats.

As expected, the mean apoptotic count from the AOM treated group was equivalent to levels measured in previous studies, including the 6h time point from 4.1.4.2. This confirmed the toxicity of the AOM and provided this study with a sound control group for which the effects of the AOM and MX treatment could be compared to.

The apoptotic results from the group administered with both the AOM and MX chemicals were of particular importance. A significantly altered apoptotic count in this group would suggest interplay between the BER system and the initiation of apoptosis.

The administration of MX did reduce the AARGC in this group, however, it was not significantly different from the AOM control group. Despite the lack of a significant difference between the apoptotic counts, there was still some evidence of an effect from the MX treatment when combined with the AOM carcinogen as seen in the reduction in the number of apoptotic cells. It is difficult however, to put this trend down to the sole effects of the inactivation of the BER pathway.

It is possible that the blocking of the BER pathway using MX may have played a role in the reduction of apoptosis. Alternatively, it is possible that the slight reduction may have simply been the result of unforseen affects of the MX chemical on the activation or effect of the AOM carcinogen. To investigate these possibilities a further more detailed investigation into the experimental design concerning the dose of agents used, the timing and number of injections and interaction between the two agents would be advised. This additional information, when compared with a measure of how efficiently the BER pathway has been interrupted, may then provide insight into the true effects of MX *in vivo* and also the role BER plays in apoptosis.

This additional information concerning the true impact of MX in the whole animal is where this small pilot study is lacking and optimisation of the study design would prove to add considerable depth to the experiment. Nevertheless, with the design having been based upon previous publications which have observed significant biological effects in mice attributed to the interruption of BER repair, it can be cautiously suggested that the findings from this study imply that the onset of acute apoptosis in colonic epithelial cells is unlikely to be solely triggered via the base excision repair pathway. In conjunction with this, these findings also imply that adducts repaired by BER, including N7meg and N3meA are unlikely to play a role in the initiation of apoptosis in the colonic epithelial cells of rats.

N7meg and 3MeA are readily formed in tissues in response to agents that are metabolised to produce alkyldiazonium intermediates [190]. While the N7meG DNA adduct causes no significant structural changes to DNA and is relatively harmless [191], the 3MeA adduct does have the potential to interfere with DNA synthesis [192]. These adducts are repaired via the DNA glycosylase Aag, which then acts to initiate the BER repair pathway. While the repair of 3MeA takes place within 24h, N7meG in particular is repaired at a very slow rate and is dependent on the level of Aag present in cells [193]. Nevertheless, regardless of the level of Aag present the BER pathway is still required for repair of these adducts to occur.

The findings of this study imply that levels of N7meg and N3meA are unlikely to play a sole role in the initiation of apoptosis. By blocking the BER pathway, the repair mechanism for these DNA adducts would have been also effectively blocked. In doing this, one can presume that the levels of these adducts would accrue in tissues. If these adducts were linked to the onset of apoptosis, this accumulative effect would likely equate to an increase in apoptosis. However, as the modulation of apoptosis was not observed in BER deficient animals, the implication of N7meg and N3meA in adduct-mediated apoptosis is not supported.

While the findings in this study were not statistically significant, there did appear to be an effect of MX on the apoptosis rate when induced by AOM. Unfortunately however, due to the size and nature of this study the biological importance of this result can not be satisfactorily interpreted and the role of the BER pathway in the apoptotic response can not be fully deduced. Therefore, while this preliminary study may provide some insight into this pathway, detailed studies are required to further investigate the true effects of the MX agent in conjunction with the AOM carcinogen in order to optimise the study design.